PUBLICATIONS OF THE ASTRONOMICAL SOCIETY OF THE PACIFIC, **124**:1124–1131, 2012 October

Speckle Camera Imaging of the Planet Pluto[1]

STEVE B. HOWELL,[2,3] ELLIOTT P. HORCH,[3,4,5] MARK E. EVERETT,[3,6] AND DAVID R. CIARDI[3,7]

Received 2012 August 16; accepted 2012 September 05; published 2012 October 3

ABSTRACT. We have obtained optical wavelength (692 nm and 880 nm) speckle imaging of the planet Pluto and its largest moon Charon. Using our DSSI speckle camera attached to the Gemini North 8 m telescope, we collected high resolution imaging with an angular resolution of ~20 mas, a value at the Gemini-N telescope diffraction limit. We have produced for this binary system the first speckle reconstructed images, from which we can measure not only the orbital separation and position angle for Charon, but also the diameters of the two bodies. Our measurements of these parameters agree, within the uncertainties, with the current best values for Pluto and Charon. The Gemini-N speckle observations of Pluto are presented to illustrate the capabilities of our instrument and the robust production of high accuracy, high spatial resolution reconstructed images. We hope our results will suggest additional applications of high resolution speckle imaging for other objects within our solar system and beyond.

1. INTRODUCTION

Pluto was discovered on 1930 February 18 by Clyde Tombaugh during his search for Planet-X, a planet lying beyond the orbit of Neptune. The planet was officially announced to the world on 1930 March 13 and named after the Greek god of the underworld. Pluto lies at an average distance from the Sun of 40 AU and has an estimated mass of 1.27×10^{22} kg. In 1978, Pluto was found to have a moon, Charon (Christy and Harrington 1978), with a diameter equal to approximately one-half that of Pluto itself. Charon's orbit is synchronous with the 6.4 day rotation period of Pluto.

Pluto's diameter is not especially well known; mutual eclipse events with its moon Charon (e.g., Young and Binzel 1994) tend to give smaller diameters, while stellar occultations (e.g., Millis et al. 1993) give larger sizes. The Millis et al. work is based on the analysis of multiple occultations and comparison to clear atmosphere and haze layer models. Their values for the solid surface of Pluto's diameter are 2390 ± 10 km (clear atmosphere) to 2370–2400 $\pm$ 10 km (haze). The radius of Pluto provided by mutual eclipse events, as discussed in Young and Binzel, independent of any limb darkening, yields a value of 2328 ± 45.8 km, which is less than that of Millis et al., albeit at the limit of agreement based on the larger uncertainty. Charon has recent diameter estimates of 1207.2 ± 2.8 km (Sicardy et al. 2006) and 1212 ± 16 km (Gulbis et al. 2006), and the ratio of the mass of Charon to Pluto is well established at 0.1165 (Tholen et al. 2008; Buie et al. 2006).

The orbit of Pluto has a high eccentricity and inclination with an orbital period of 248 yr; Pluto is in a 3:2 resonance with the orbit of Neptune. Pluto has a relatively high mean albedo in the optical when compared to smaller Kuiper belt objects and many icy satellites, although it does have dark regions and shows phase variations throughout its 6.4 day rotation period (see Buie et al. 2010; Buratti et al. 2003; Young et al. 1999; Reinsch et al. 1994). Pluto is now known to have five moons, the latest discovered very recently in 2012 July. The four newer moons are very small bodies orbiting Pluto with periods of 20–30 days and visual magnitudes of twenty-fourth and fainter. The NASA *New Horizons* mission is scheduled to visit Charon and Pluto in 2015 July, making new high-resolution observations of the system particularly timely over the next couple of years.

Observations of Pluto and Charon are difficult due to their faintness (~14th and ~16th visual magnitude, respectively), as well as their mean angular separation of only ~0.8″. Their sizes can be resolved in the highest resolution images, revealing typical angular diameters of 0.11″ for Pluto and 0.05″ for Charon. Speckle imaging of Pluto was attempted over two decades ago by a number of observers, mainly in order to determine the

[1] Based on observations obtained at the Gemini Observatory, which is operated by the Association of Universities for Research in Astronomy, Inc., under a cooperative agreement with the National Science Foundation on behalf of the Gemini partnership: the National Science Foundation (United States), the Science and Technology Facilities Council (United Kingdom), the National Research Council (Canada), CONICYT (Chile), the Australian Research Council (Australia), Ministério da Ciência, Tecnologia e Inovação (Brazil) and Ministerio de Ciencia, Tecnología e Innovación Productiva (Argentina).

[2] NASA Ames Research Center, Moffett Field, CA 94035.

[3] Visiting Astronomer, Gemini-North Telescope, 670 North Aohoku Place, Hilo, HI.

[4] Department of Physics, Southern Connecticut State University, 501 Crescent Street, New Haven, CT 06515.

[5] Adjunct Astronomer, Lowell Observatory, 1400 West Mars Hill Road, Flagstaff, AZ 86001.

[6] National Optical Astronomy Observatory, 950 North Cherry Avenue, Tucson, AZ 85719.

[7] NASA Exoplanet Science Institute, California Institute of Technology, Pasadena, CA 91125.

orbital parameters for Charon. Hetterich & Weigelt (1983) and Baier & Weigelt (1987) used an image intensifier, photon-counting camera for their speckle work, and their papers summarize the field at the time. These authors were able to determine Charon's separation and position angle to near $0.025''$ and 1°–2°, respectively, using autocorrelation techniques. Baier & Weigelt (1987) even set out to determine the diameters of Pluto and Charon by modeling the source flux distribution in an attempt to reproduce the autocorrelations they obtained. The diameter estimates had nearly a 50% uncertainty. During the 1984–1985 season, Beletic et al. (1989) performed speckle observations of Pluto in order to better define Charon's orbit. Their work used a two-dimensional image intensifier that typically received 30 photons in each Pluto speckle image. They also produced a reconstructed image of Pluto and Charon using 18,000 speckle frames but did fully resolve the two bodies enough to allow diameter measurements.

Given that it is a challenge to obtain an image of the Pluto-Charon system with sufficiently good spatial resolution to measure its orbital and physical parameters, we chose to observe these bodies as a test of our speckle camera performance. The results discussed below demonstrate the capabilities of our hardware and software in terms of magnitude limits and resolution. We hope that the results will spark other ideas for the application of speckle imaging.

We observed Pluto with our speckle camera system using the Gemini North (Gemini-N) 8 m telescope. Our camera is a visiting instrument making its first voyage to Gemini. We describe below the observational setup and our speckle imaging techniques, which differ slightly from our previous efforts (see Howell et al. 2011; Horch et al. 2009, 2011). We follow this with our results for the Pluto-Charon system. We discuss our camera's abilities, as well as its limitations, for such work and end with some conclusions about future improvements and possibilities for additional speckle imaging applications.

2. GEMINI SPECKLE OBSERVATIONS AND TECHNIQUES

We observed Pluto using our Differential Speckle Survey Instrument (DSSI) camera (Horch et al. 2009, 2011; Howell et al. 2011) at the Gemini-N 8 m telescope located on the 4,200 m summit of Mauna Kea on the Big Island of Hawaii. As a visitor instrument, DSSI was mounted on a side-looking Cassegrain port (see Fig. 1). The installation went smoothly using a customized interface box and the expert help of the Gemini-N day crew.

The DSSI speckle camera uses a dichroic element to split the beam into red and blue channels, sending single channels to each one of our two 512×512 pixel Andor Ixon electron multiplying CCD (EMCCD) cameras. Prior to the dichroic, the beam passes through a collimating lens. The dichroic is then followed by a bandpass filter and a magnifying (reimaging) lens to focus the image on each detector. We used filters with

FIG. 1.—Photograph of DSSI mounted on the side port at Gemini-N. The instrument (*silver box with two cameras attached*) is surrounded by the larger, standard Gemini instrument cage enclosure.

central wavelengths of 692 nm and 880 nm and bandpass widths of 40 nm and 50 nm, respectively. This configuration resulted in plate scales of $^{0.010859}/\!/$ pixel^{-1} and $^{0.011366}/\!/$ pixel^{-1} in the 692 nm and 880 nm channels, respectively. These plate scales were designed to produce nearly Nyquist sampling for point sources imaged at the diffraction limit of an 8 m telescope.

The observing techniques we used to image Pluto were essentially the same as we normally use for speckle imaging of stars. We observed Pluto on 2012 July 28 from 9:00 to 9:36 UT near the meridian at an airmass of 1.3. As always, we also observed a nearby single star to serve as a point source calibrator for image reconstruction. The native seeing at the time is estimated from our data to have been 0.4" full width at half-maximum (FWHM). With the telescope guided and tracking Pluto, we obtained eight sets of 1000 frame, 60 ms exposures of the Pluto-Charon system simultaneously in each filter (total exposure time for each filter was 8 min). Our observations of the fifth magnitude calibrator star consisted of one set of 1000 60 ms frames in each filter. In each camera, we selected a 256×256 pixel subregion centered on either Pluto or the point source calibrator for read outs. This resulted in a $2.8'' \times 2.8''$ field of view. A typical 60 ms, 692 nm speckle frame from the Pluto data is shown in Figure 2.

The speckle instrument settings for Gemini were quite similar to those we have used at the Wisconsin-Indiana-Yale-NOAO (WIYN) 3.5 m telescope (Howell et al. 2011), but with the pixel scale approximately 2 times smaller in order to produce similar point spread function (PSF) sampling when accounting for the ratio of the diffraction limits on the two telescopes. Our field of view at Gemini was approximately the same size as for WIYN because we chose to read out

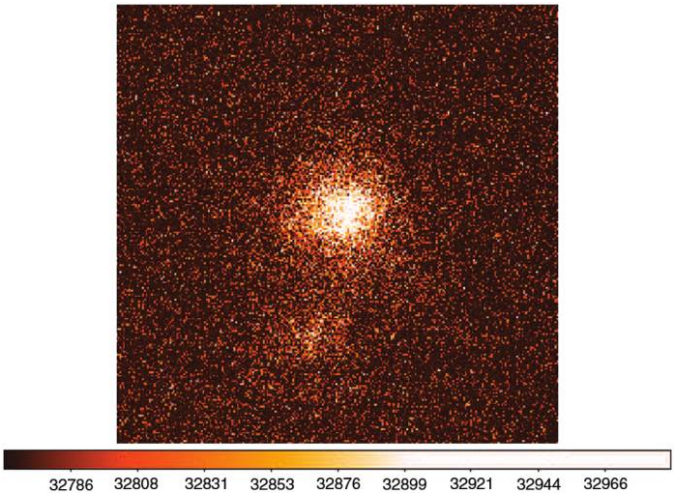

FIG. 2.—One of our typical 692 nm filter, 60 ms speckle frames obtained with the Gemini telescope. Pluto and Charon can both be seen here as relatively faint, extended speckle images. Speckle integration times are matched to the estimated atmospheric correlation times believed to be present above the telescope in an effort to balance the collection of more photons with the ability to use very short exposures in order to freeze the atmospheric distortions. The color bar gives the pixel values, in counts, for the image.

regions with twice the width on the detector. The field size in either case matches typical widths for the isoplanatic patch, beyond which the seeing effects on two sources become decorrelated and speckle imaging techniques are less effective.

Observing at Gemini with the DSSI presents some relevant differences versus speckle observing at WIYN, however. The median seeing at Gemini in the R-band is $\sim 0.6''$ FWHM, compared with $\sim 0.8''$ at WIYN. This means that the correlation time of the atmosphere is longer at Gemini, and it was therefore appropriate to use a longer frame integration time. At WIYN, we typically use 40 ms; for the observations discussed here, we chose 60 ms. Because of the larger aperture, we had 5.35 times the light that we collect at WIYN in the same filter; but, because of the larger telescope size, there are also more speckles produced on the image plane. Obviously, the large aperture gives the benefits of more total photons per unit time and higher resolution.

To precisely determine our plate scale and instrument rotation, we observed two binary stars with extremely well-known orbits. An estimate of our astrometric precision differences between the 692 and 880 nm observations, as well as the uncertainties in the positions based on the binary star orbital ephemerides, is 2 mas in separation and 0.4° in position angle. More detail on the astrometric calibration for the run will appear in Horch et al. (2012), in which we will discuss the binary stars and *Kepler* mission exoplanet targets observed during the run.

3. RESULTS

According to the JPLHORIZONS estimate,[8] Pluto was at a V magnitude of 14.0, while Charon was fainter at $V = 15.9$ during the time of our Pluto-Charon observations. The angular separation and position angle of Pluto and Charon were predicted to be $0.81''$ and 169.5°, respectively. Pluto itself was expected to produce a resolved angular disk $0.105''$ in diameter, while Charon would be smaller with an angular diameter of $0.053''$.

The speckle data frames were processed with our existing reduction programs; these involve computation of the spatial frequency power spectrum and near axis subplanes of the bispectrum, as discussed in previous papers (Horch et al. 2009, 2011). In order to determine the relative astrometry of the two bodies, we treated the system as if it were a binary star and used our normal power spectrum fringe fitting routine to arrive at the position angle and separation of Charon and Pluto. Because the two bodies are disks and not point sources, the fringes do not extend to the diffraction limit in the Fourier plane; to compensate for this, we masked the power spectrum with a circular mask that was only slightly larger than the spatial frequency at which the fringes died away and performed the binary fit only inside this region. When done on both the 692 and 880 nm data, the results of this procedure agreed within 0.1° in position angle and within 0.2 mas in separation between the two filters. The final position angle and separation values are shown in Table 1. We note that the albedo patterns on Pluto can throw off the relative astrometry in systematic ways as a function of the orbital longitude (e.g., Tholen et al. 2008; Buie et al. 2012).

We can also determine the magnitude difference between the two sources based on the power spectrum fit. The ratio of the geometric albedos is approximately constant between Pluto and Charon in our two bandpasses: 2.02 (692 nm) and 2.20 (880 nm) (Fink and DiSanti 1988). We note that our narrow 880 nm filter avoids the CH_4 absorption band in Pluto's spectrum. Table 1 contains our determined magnitude difference values. We have previously studied the uncertainty of magnitude differences in our speckle work with the same instrument at WIYN; using Figure 7 in Horch et al. (2010) as a guide, rough uncertainties for these values are probably in the ± 0.15 mag range for each of our two filters.

From the power spectra and bispectra, we computed a final reconstructed image in both filters. These are shown in Figure 3, where the images clearly show that both bodies are resolved. The 880 nm image was of lower quality than the 692 nm image due to its intrinsically lower resolution (longer wavelength) and the fact that the measured fluxes were lower at the longer

[8] The HORIZONS model magnitude accounts for Pluto's phase angle and distance from the Sun and observer, but not its light curve. Pluto's light curve has a ~ 0.2 mag amplitude (Buie et al. [2010]) that is not accounted for here. The JPL HORIZONS on-line solar system data and ephemeris computation service is available at http://ssd.jpl.nasa.gov/?horizons.

TABLE 1
PLUTO-CHARON RELATIVE ASTROMETRY

Parameter	Predicted Value[a]	Speckle Results[b] 692 nm	880 nm	Average
Separation (mas)	810 ± 2	805.1	804.9	805.0 ± 2
Position Angle (deg)	169.5 ± 0.5	171.1	171.1	171.1 ± 0.4
Magnitude Difference (mag)	1.87 ± 0.2	1.7	1.8	1.75 ± 0.15

[a] Based on HORIZONS ephemerides (and uncertainties) calculated for observations from the Gemini-N observatory on 2012 July 28 at 8:29 UT. Our speckle observations were made during the time period of 9:00 to 9:36 UT.

[b] Despite the agreement here between the two filters, binary star measurements indicate that the speckle results have an uncertainty of ~2 mas for separation and ~0.4° for position angle.

wavelength. Considering the falloff in quantum efficiency of the detector between 692 and 880 nm, as well as the reduction in solar flux and other factors, the count rate in the 880 nm band was only about one third of that in the 692 nm filter. In both images, two known artifacts of the image reconstruction process have been estimated and removed. First, when reconstructing faint sources, our bispectral method can produce a spike at the center of the image that resembles a point source. We removed this by dividing the image with a scaled version of a reconstructed image of a point source added to a frame with unit value in all pixels (Fig. 3). Thus, the spike is suppressed while pixel values in other parts of the image are unchanged.

Second, lower signal-to-noise ratio (S/N) reconstructions sometimes exhibit a faint "cross" pattern aligned with pixel axes; this is related to the de-biasing of each speckle frame prior to further reduction. We have removed this as much as possible by noting that the signature of the cross in the Fourier plane is also a cross pattern, and we have replaced the value of pixels in the cross in the Fourier plane with an average of nearest neighbor pixels orthogonal to the cross at each point.

In the resulting 692 nm image, the background noise around Charon is approximately 4% of the mean flux in the disk of the moon itself, suggesting that our 3σ detection limit (for a point source) in this reconstructed image is approximately magnitude 18.9. (The value in the 880 nm image is not as faint, owing to the lower S/N.) Therefore, we would not expect to see any of Pluto's other moons even if they were within the frame, due to their faintness (e.g., Weaver et al. 2006).

In order to measure diameters, we computed the derivatives along cuts in the image that bisect Pluto and Charon respectively. The absolute value of the derivative along such a cut displays two local maxima on each edge of the disk of the body. By measuring the separation between these points, we can estimate the diameter of each body. Since the "cross" pattern mentioned

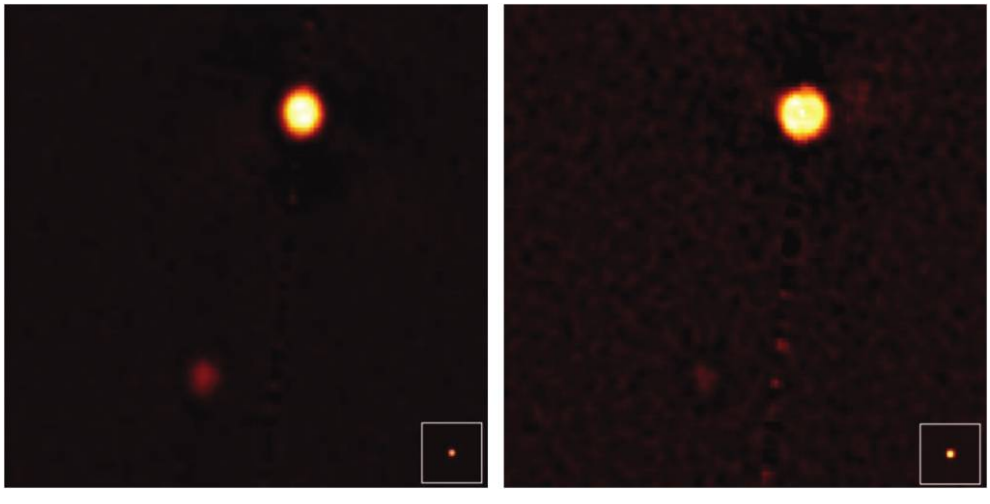

FIG. 3.—Our final speckle image reconstructions of Pluto and Charon. *Left*: The image obtained at 692 nm. *Right*: The image obtained at 880 nm. In both plots, north is up, east is to the left, and the image section shown here is $1.39'' \times 1.39''$. No pixel smoothing has been applied to this image and the low-level "line pattern" (*near vertical and mainly visible in the 880 nm image*) centered on Pluto is an artifact of the speckle image reconstruction process. Intensity variations seen on the resolved disks are most likely noise from the image reconstruction process. *Lower right* insets show a reconstructed point source.

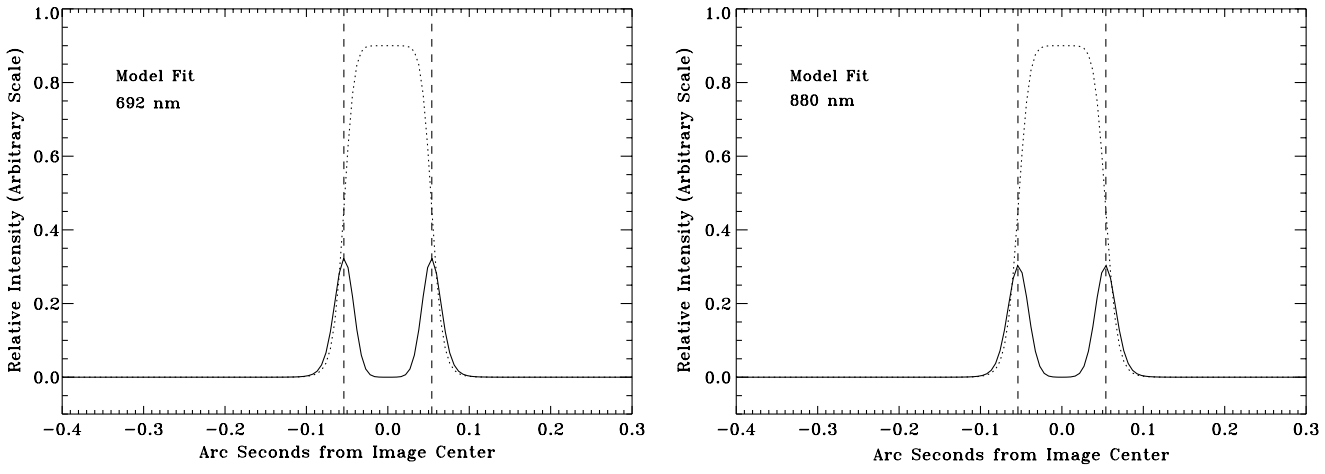

FIG. 4.—Cuts through model images, showing the diameter estimation procedure. The image profile is shown as a dotted line, the absolute value of the derivative of the image profile is shown as a solid line, and the vertical dashed lines mark the maxima of the derivative on either side of the image center. In both cases, the input disk diameter was correctly obtained by measuring the distance between the two dashed lines.

above did not completely subtract away, we have computed derivatives in directions of 45° and 135° relative to the pixel coordinates (that is, along diagonals), to minimize any contributions due to noise spikes in the cross. Before using this method on the data in Figure 3, we first tried it on rounded (Butterworth profiles, Gonzalez and Woods [2002, p. 173]) and flat disk models of known diameters, convolved with our expected PSF, and found the derived diameter to match the input diameter to better than 0.5% in all trials, regardless of the details of the shape of the disk. An example of these model fits is shown in Figure 4. Note, we did not use a Lambertian profile, even though it too has a maximum derivative at the radius of an object. Such a profile can lead to an underestimate of the true radius, due to the edge softening as a result of its cosine nature, and it is also not clear that this sort of profile is appropriate to use in this case, given the known albedo variations. The use of a possibly non-realistic model profile may lead to a small systematic uncertainty in our radii, but we feel this is negligible due to our very high resolution images.

Plots illustrating the diameter fitting for Pluto are shown in Figure 5 for the 692 nm image and in Figure 6 for the 880 nm image. Both sources are fainter, providing slightly lower S/N results, in the 880 nm images. By averaging the two values, we obtain our diameter results for the two bodies, along with an uncertainty, as determined from the standard error of the four

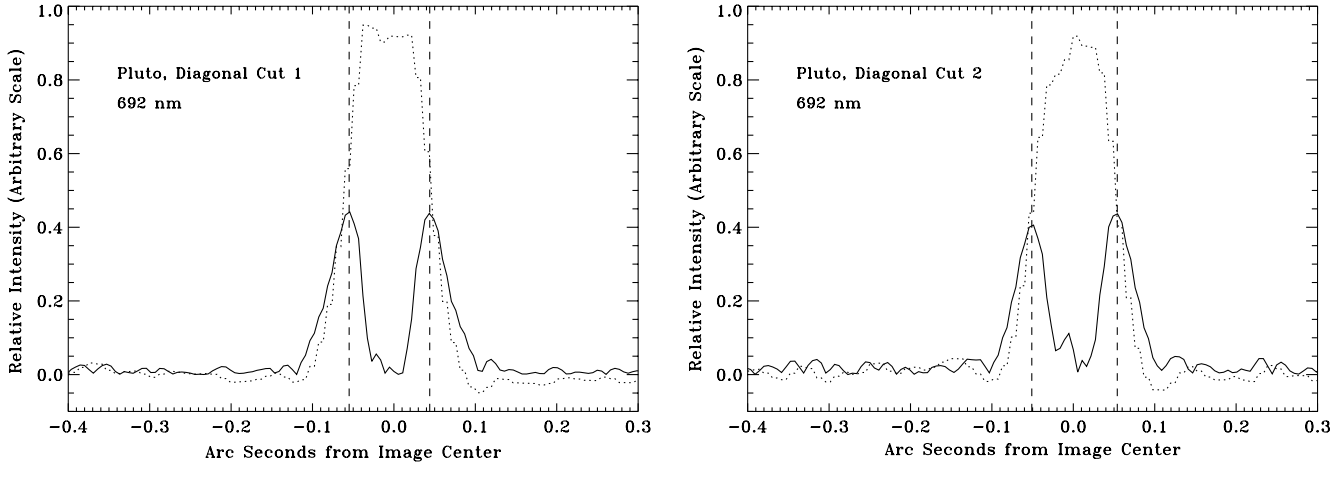

FIG. 5.—Cuts diagonal to the pixel axes through the 692 nm image of Pluto. As in the previous figure, the image profile is shown as a dotted line, the absolute value of the derivative of the image profile is shown as a solid line, and the vertical dashed lines mark the maxima of the derivative on either side of the image center.

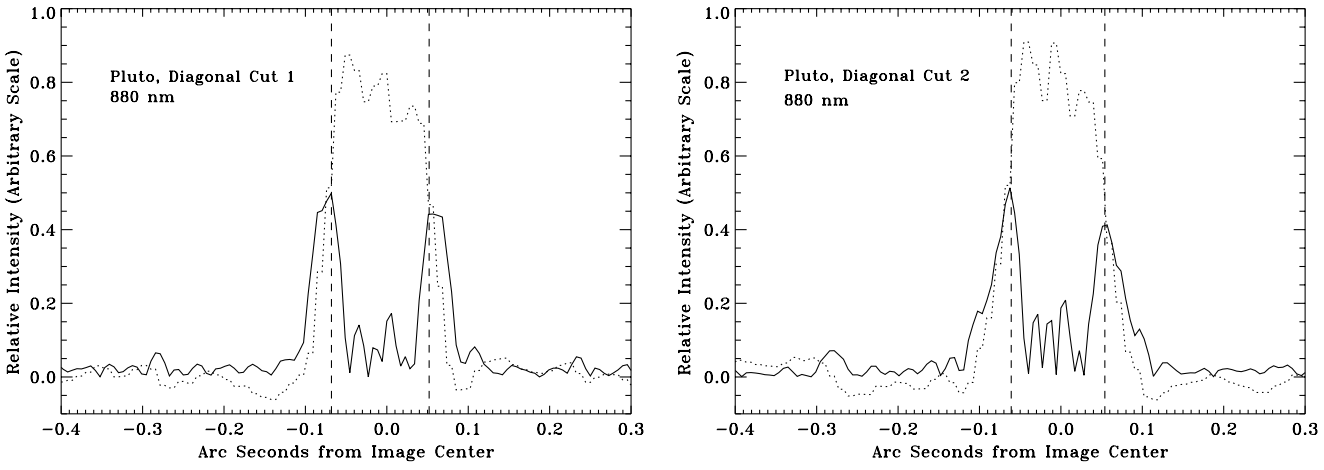

FIG. 6.—Cuts diagonal to the pixel axes through the 880 nm image of Pluto. As in the previous figures, the image profile is shown as a dotted line, the absolute value of the derivative of the image profile is shown as a solid line, and the vertical dashed lines mark the maxima of the derivative on either side of the image center.

independent values (that is, two in each filter). Our final values are presented in Table 2.

For Charon, one final image correction was made prior to estimating the diameter. We have noticed in our past speckle observing that when the image reconstruction is formed for a low S/N observation of a secondary in a binary star system (i.e., a faint companion), the FWHM of the faint companion is larger by a small amount than that of the primary (brighter) source. While the effect warrants more study, we believe that this is due to slight decorrelation of the speckles between the primary and secondary sources. This fact suggests that, in the case of the sixteenth magnitude Charon, we should anticipate that the value of the diameter obtained from the raw reconstructed image would be slightly overestimated. To quantify this effect, we examined the FWHM of two relatively faint binary stars with very faint, low S/N secondaries observed during our Gemini run and determined that the ratio of the secondary to primary FWHM is approximately1.36 ± 0.15. We assumed that the Charon image is affected in the same way and divided our raw diameter measurement as described above by this same factor. The final diameters for Charon are shown in Table 2, and plots illustrating the diameter measurements are shown in Figures 7 and 8. Our final measurements for the diameters of both Pluto and Charon agree well with the currently-known values.

TABLE 2

PLUTO-CHARON ANGULAR DIAMETERS[a]

Source	Pluto (mas)	Charon (mas)
HORIZONS[b]	105 ± 1	53 ± 0.5
Millis et al. (1993)	108.9 ± 0.5	...
Young & Binzel (1994)	106.2 ± 2.1	...
Gulbis et al. (2006)	...	55.3 ± 1.4
Sicardy et al. (2006)	...	55.1 ± 0.2
Speckle (692 nm)	102	58
Speckle (880 nm)	117.5	56.5
Speckle Avg.	109.7 ± 4.8	57.2 ± 7.2

[a] At the time of our observations, 1 mas = 21.92 km at the distance of Pluto.

[b] Based on HORIZONS ephemerides and uncertainties.

4. CONCLUSIONS

We have used the Gemini-N 8 m telescope with our DSSI speckle camera to observe the planet Pluto and its largest moon Charon. Our results for the relative astrometry of Charon's separation and position angle are given and agree with the best ephemeris values. If additional speckle observations of the Pluto-Charon system would show that parameter determination is insensitive to albedo patterns, further speckle observations may be a valuable addition to the orbit determination. Furthermore, we have produced the first fully-resolved, reconstructed speckle image of Pluto and Charon that resulted in measurements of their angular diameters. The measured angular diameters of Pluto and Charon are equal to the current best values to within ~3–4 mas, respectively. Speckle observations could potentially contribute to resolving the occultation versus mutual event diameter uncertainty prior to the encounter by *New Horizons* in 2015.

The speckle observations discussed here, produced results essentially in agreement with our pre-observation expectations. Our EMCCD cameras have typical sensitivities throughout the optical range, and various choices of the two filters to use for specific simultaneous observations are easily accommodated. Additional improvements to our reduction pipeline, such as production of model point sources and handling of sky background reconstruction, suggested themselves, and we have initiated

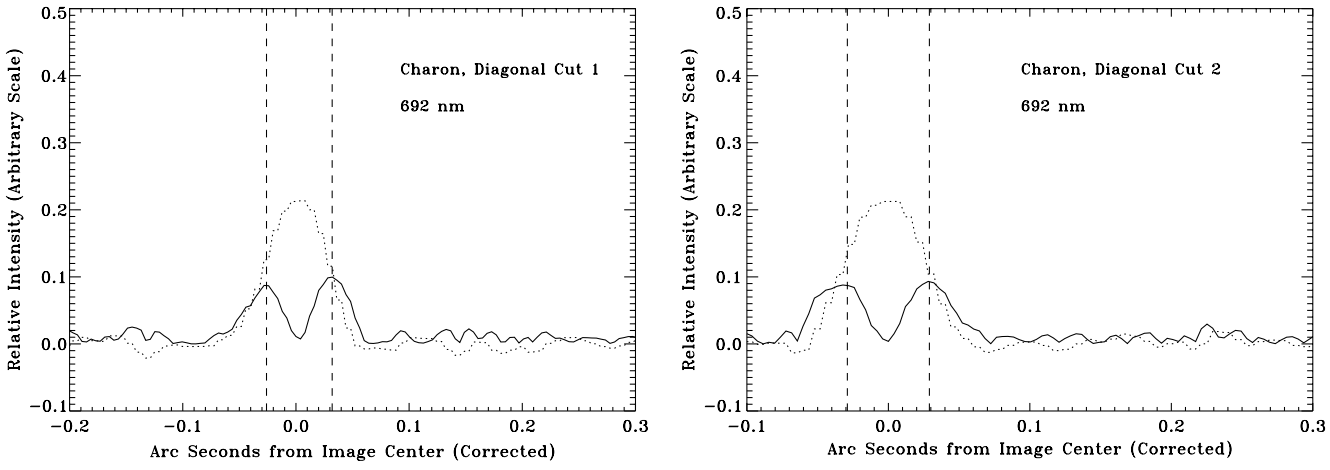

FIG. 7.—Cuts diagonal to the pixel axes through the 692 nm image of Charon. As in the previous figures, the image profile is shown as a dotted line, the absolute value of the derivative of the image profile is shown as a solid line, and the vertical dashed lines mark the maxima of the derivative on either side of the image center.

plans to study alternative software approaches in these areas. Given the ability to produce fully resolved, high resolution optical images with our speckle camera, we believe that solar system studies of other objects (e.g., binary asteroids, rotation and shape determination, astrometric orbits) are warranted. Speckle observations of additional astronomical objects, such as star cluster cores or astrophysical jets, would be excellent targets as well.

The ground-based observations reported on herein were obtained at the Gemini-N observatory as part of Gemini Science Program GN-2012A-DD-8. The authors wish to thank Andy Adamson, Inger Jorgensen, Steve Hardash, Andrew Stephens, Katherine Roth, Jennifer Holt, Jonathan Kemp, Jesse Ball, Tony Matulonis, Harlan Uehara, Cooper Nakayama, Rody Kawaihae, James Franco, Chris Yamasaki, Cy Bagano, Simon Chan, Mike Becher, Tim Minick, Joseph D'Amato, John White, Arturo Nunez, Fred Chaffee, and Nancy Levenson of Gemini-N without whom our visit and results could not have been possible. Bill Merline kindly provided us with the calculated parameters for Pluto and Charon during the time of our observations. We want to extend a special thank you to the anonymous referee whose expertise in Pluto and Charon, as well as their complete review, helped make this a better paper. This research work was partially funded by the NASA *Kepler* discovery mission.

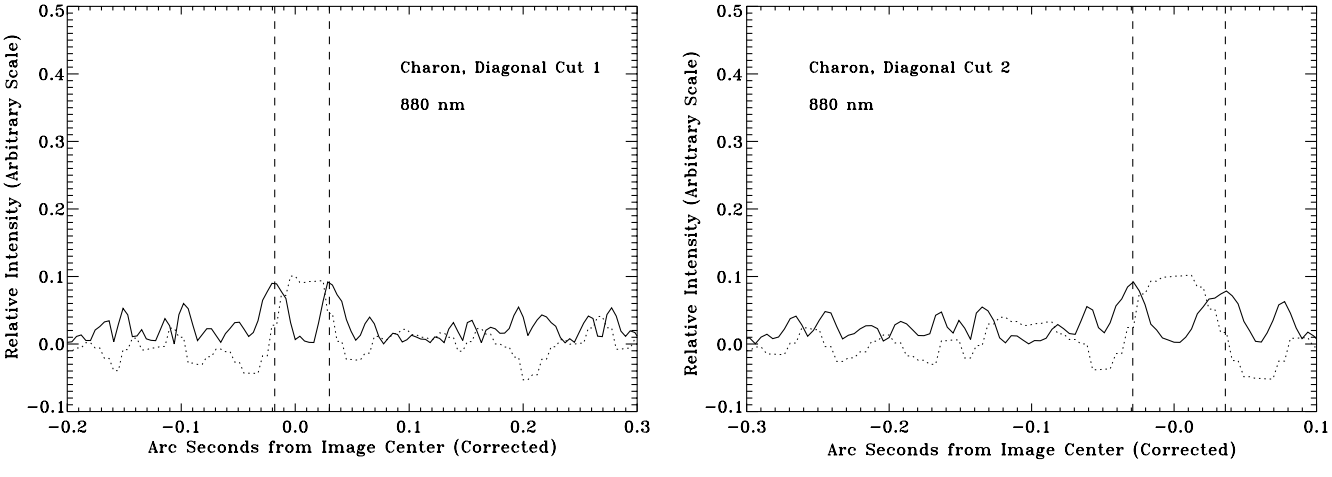

FIG. 8.—Cuts diagonal to the pixel axes through the 880 nm image of Charon. As in the previous figures, the image profile is shown as a dotted line, the absolute value of the derivative of the image profile is shown as a solid line, and the vertical dashed lines mark the maxima of the derivative on either side of the image center.

REFERENCES

Baier, G., & Weigelt, G. 1987, A&A, 174, 295

Beletic, J. W., Goody, M., & Tholen, D. J. 1989, Icarus, 79, 38

Buie, M. W., Grundy, W. M., Young, E. F., Young, L. A., & Stern, S. A. 2006, AJ, 132, 290

———. 2010, AJ, 139, 1128

Buie, M. W., Tholen, D. J., & Grundy, W. M. 2012, AJ, 144, 15

Buratti, B. J., et al. 2003, Icarus, 162, 171

Christy, J. W., & Harrington, R. S. 1978, AJ, 83, 1005

Fink, U., & DiSanti, M. 1988, AJ, 95, 229

Gonzalez, R. C., & Woods, R. E. 2002, Digital Image Processing (Upper Saddle River: Prentice Hall)

Gulbis, A. A. S., et al. 2006, Nature, 439, 48

Hetterich, N., & Weigelt, G. 1983, A&A, 125, 246

Horch, E. P., Howell, S. B., Everett, M. E., Ciardi, D. R., 2012, AJ, submitted

Horch, E. P., Falta, D., Anderson, L. M., DeSousa, M. D., Miniter, C. M., Ahmed, T., & van Atena, W. F. 2010, AJ, 139, 205

Horch, E. P., Gomez, S. C., Sherry, W. H., Howell, S. B., Ciardi, D. R., Anderson, L. M., & van Altena, W. F. 2011, AJ, 141, 45

Horch, E. P., Veillette, D. R., Gallé, R. B., Shah, S. C., O'Reilly, G. V., & van Altena, W. F. 2009, AJ, 137, 5057

Howell, S. B., Everett, M. E., Sherry, W., Horch, E., & Ciardi, C. 2011, AJ, 142, 19

Millis, R. L., et al. 1993, Icarus, 105, 282

Reinsch, K., Burwitz, V., & Festou, M. C. 1994, Icarus, 108, 20

Sicardy, B., et al. 2006, Nature, 439, 52

Tholen, D. J., Buie, M. W., Grundy, W. M., & Elliott, G. T. 2008, AJ, 135, 777

Young, E., & Binzel, R. P. 1994, Icarus, 108, 219

Young, E. F., Galdamez, K., Buie, M. W., Binzel, R. P., & Tholen, D. J. 1999, AJ, 117, 1063

Weaver, H. A., et al. 2006, Nature, 439, 943